Hindawi
Geofluids
Volume 2022, Article ID 7430025, 12 pages
https://doi.org/10.1155/2022/7430025

Research Article

Pressure Relief and Permeability Enhancement Mechanism of Short-Distance Floor Roadway in Deep Coal Roadway Strip

Benqing Yuan,[1,2,3,4] **Min Tu**,[1,3] **Jianjun Cao**,[2,4] **and Xiang Cheng**[1]

[1]*State Key Laboratory of Mining Response and Disaster Prevention and Control in Deep Coal Mines, Anhui University of Science and Technology, Huainan 232001, China*
[2]*CCTEG Chongqing Research Institute, Chongqing 400037, China*
[3]*Key Laboratory of Safety and High-Efficiency Coal Mining of Ministry of Education, Anhui University of Science and Technology, Huainan 232001, China*
[4]*State Key Laboratory of the gas Disaster Detecting, Preventing and Emergency Controlling, Chongqing 400037, China*

Correspondence should be addressed to Benqing Yuan; bqyuan@aust.edu.cn, Min Tu; mtu@aust.edu.cn, Jianjun Cao; 108485815@qq.com, and Xiang Cheng; xcheng@aust.edu.cn

Received 20 September 2021; Accepted 24 February 2022; Published 24 March 2022

Academic Editor: Zhijie Wen

A pressure relief and permeability enhancement method through short-distance floor roadway was proposed to solve the difficult outburst prevention during the gas extraction at the coal roadway strips in deep outburst coal seams with high ground stress and low gas permeability. On the basis of an equivalent model of the surrounding rock in a deep roadway, the analytical solutions of deep roadway excavation to the stress and deformation of pressure relief at overlying short-distance coal roadway strips were obtained using the unified strength theory and nonassociated flow rules. Next, the criteria for determining the reasonable position of floor roadway were established, and a mechanical model of short-distance floor roadway for the pressure relief and permeability enhancement zone at the overlying coal seam was constructed. Finally, the scope of the zonal disintegration at the coal roadway strips in the elastic and elastic–plastic zones of the surrounding rock in the roadway, as well as the expression of gas permeability change, was given. The engineering trial calculation and practice showed that the stress and strain of the surrounding rock in the roadway were evidently influenced by the intermediate principal stress coefficient. Moreover, the vertical stress and vertical displacement of overlying coal seam were gradually reduced with the increase in the intermediate principal stress coefficient and vertical distance of the floor roadway. The minimum reasonable distance arranged for the 213 floor roadway in Qujiang Coal Mine was 6.21 m, and the effective pressure relief should be conducted within 10.6 m from the coal seam floor. When the pressure relief was located at 9.0 m from the coal seam floor, the investigation results were basically consistent with the theoretical analysis results, exerting obvious pressure relief and permeability enhancement effects on the overlying short-distance coal roadway strips.

1. Introduction

Coal is the basic energy source that guarantees the energy safety and stability in China. Coal resources are estimated to still account for over 50% of primary energy consumption by 2030 [1, 2]. China is also one of the countries with the most serious coal and gas outburst (hereinafter abbreviated as "outburst") in the world, and the main regional measures taken to prevent and control the outburst include the exploitation of the protective layer and gas preextraction at the coal seam. For the single outburst coal seam or coal seam group without exploitation of the protective layer, the coal roadway strips at the outburst coal seam will be initially exploited, and the outburst prevention measure is still mainly to drill the crossing holes on the floor roadway for the gas preextraction [3–5].

However, with the continuously increasing coal mining depth in China, the high ground stress and low gas permeability of outburst coal seams in most coal mines are more prominent. The difficulty in the drilling construction under

deep high ground stress condition is significantly aggravated, and the gas preextraction further enhances the ground stress-dominated dynamic danger [6, 7], such as the ground stress-dominated dynamic disasters appearing in deep mines in provinces such as Anhui, Liaoning, and Jiangxi. Hence, pressure relief and permeability enhancement technologies, such as hydrofracturing, hydraulic reaming, and control of presplitting blasting, have been investigated in coal mines in China [8–14]. However, some shortcomings exist, such as large difference in the effect of pressure relief and permeability enhancement, failure to change the stress condition of surrounding rock in advance, and complex process.

Given the complex and diversified stress field evolution of the surrounding rock in deep roadways, the large deformation and strong rheological properties of surrounding rock, the brittleness–ductility transformation of coal and rock mass, and the mutability of dynamic response [15, 16], an elastic–plastic deformation model of the surrounding rock in deep roadway was constructed to study the mechanical mechanism of a preexcavated short-distance floor roadway for the pressure relief of the surrounding rock and the permeability enhancement of the overlying coal seam. Next, the proactive pressure relief and permeability enhancement method for the short-distance floor roadway at the coal roadway strips in the deep outburst coal seams with high ground stress and low gas permeability was established, expecting to provide a reference for the outburst prevention and control at the coal roadway strips in deep mines.

2. Deformation Analysis of Layered Surrounding Rock in Deep Roadway

2.1. Equivalent Model Construction for Overlying Layered Rock Strata in Roadway. In engineering practice, the deep surrounding rock in a roadway is kept stable under the load effect of the vertical strata at the roof, and the displacement and section rotation of rock beam at the roof are restricted by the clamping effect between the rock strata. Under this circumstance, the upper rock stratum of the roadway can be simplified into a mechanical constraint model of a simply supported beam (Figure 1).

As shown in Figure 1, the bending moment at the support x is

$$M_x = \frac{1}{2}\mathrm{qlx} - \frac{1}{2}\mathrm{qx}^2 + \mathrm{p}\omega - M, \tag{1}$$

where l is the upper rock beam span of the roadway, m; p stands for the horizontal force at the fixed end, $p = \lambda q b_0 h$, MPa; λ is the lateral pressure coefficient of the rock beam; b_0 denotes the width of the rock beam, m; ω is the deflection of the rock beam; and M is the bending moment at the support.

According to the principle of static equilibrium, a differential equation can be listed as follows:

$$\omega'' + \frac{P}{\mathrm{EI}}\omega = -\frac{\mathrm{ql}}{2\mathrm{EI}}\mathrm{x} + \frac{q}{2\mathrm{EI}}\mathrm{x}^2 + \frac{M}{\mathrm{EI}}. \tag{2}$$

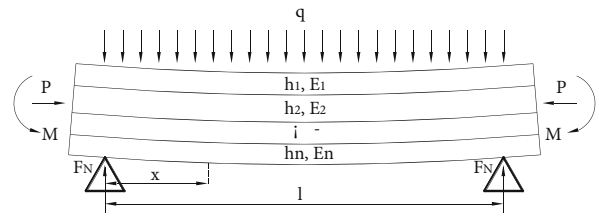

Figure 1: Hierarchical mechanical analysis chart of two-end simple support constraints.

$\mathrm{P/EI} = \beta^2$ is set, and the differential equation is solved to obtain

$$\omega = A\sin\beta x + B\cos\beta x + \frac{q}{2p}x^2 - \frac{q\mathrm{l}}{2p}\mathrm{x} + \frac{M_B}{p} - \frac{q}{p\beta^2}. \tag{3}$$

The boundary conditions $\begin{cases} x = 0 & \omega = 0 \quad \theta = 0 \\ x = \mathrm{l} & \omega = 0 \quad \theta = 0 \end{cases}$ are substituted into the above equation to solve

$$\begin{cases} A = \left(\dfrac{q}{p\beta^2} - \dfrac{M}{p}\right)\tan\dfrac{\beta\mathrm{l}}{2} \\ B = \dfrac{q}{p\beta^2} - \dfrac{M}{p} \\ M_B = \dfrac{q}{\beta^2} - \dfrac{q\mathrm{l}}{2\beta}\cot\dfrac{\beta\mathrm{l}}{2} \end{cases}. \tag{4}$$

According to the deformation continuity condition in mechanics, the deformation of each rock stratum is continuous in the vertical direction, that is, the rock strata share the same deflection, that is, $\omega = \omega_1 = \cdots\cdots = \omega_\mathrm{i}$. In actual working conditions, the mutual bonding power between rock strata is extremely weak that it can be neglected. Then,

$$\omega_0 = \frac{q\mathrm{l}}{2p\beta}\tan\frac{\beta\mathrm{l}}{4} - \frac{q\mathrm{l}^2}{8p} = \omega_i = \frac{q_i l}{2p_i\beta_i}\tan\frac{\beta_i\mathrm{l}}{4} - \frac{q_i l^2}{8p_i}, \tag{5}$$

where ω_0 is the bending moment at the midspan of the rock beam; and q_i and p_i represent the vertical load and end horizontal acting force borne by the layer i, respectively, MPa.

Assume that the total height of the rock beam is h, and the horizontal acting force at the end of the rock beam of layer i is $p_i = (h_i/h)p$. For a specific rock stratum, Equation (5) can be simplified as follows:

$$\frac{4}{\beta}\tan\frac{\beta\mathrm{l}}{4} = \xi, \tag{6}$$

where ζ is the constant of a specific rock stratum.

Variable β cannot be separated from the left end of Equation (6), and its numerical solution can be solved through programming. According to $\mathrm{p/EI} = \beta^2, p = \lambda q b_0 h$, and the sectional inertia moment $I = b_0 h^3/12$ of the rock

beam, the overall equivalent elasticity modulus of the rock strata above the roadway is

$$E = \frac{12\lambda q}{h\beta^2}. \tag{7}$$

2.2. Elastic–Plastic Deformation Analysis of Surrounding Rock in Deep Roadway. The elastoplasticity and brittleness of the surrounding rock in roadway have been analyzed by most scholars using the Mohr–Coulomb criterion or Hoek–Brown criterion [17, 18], but the effect of intermediate principal stress has not been considered. As pointed out in literature [19, 20], given that the failure strength of a rock is strengthened due to the intermediate principal stress, an obvious disintegration zone with poor mechanical properties of rocks appears in the surrounding rock excavated in the deep roadway with high ground stress.

On this basis, the surrounding rock in a deep roadway was divided into elastic, plastic, and disintegration zones in this study based on the unified strength criterion and nonassociated flow rule to analyze the limiting equilibrium. To facilitate the calculation, a circular roadway was taken for example to establish a mechanical model (Figure 2) of the surrounding rock in this deep circular roadway, and the whole stress–strain curves of the rock were simplified, as shown in Figure 3.

The differential equation of the equilibrium that the stress in each zone should meet (body force unconsidered) is

$$\frac{d\sigma_r}{\mathrm{dr}} + \frac{\sigma_r - \sigma_\theta}{r} = 0. \tag{8}$$

The geometric equation is

$$\begin{cases} \varepsilon_r = \dfrac{\partial \mathrm{u}}{\partial \mathrm{r}} \\ \varepsilon_\theta = \dfrac{u}{r} \end{cases}. \tag{9}$$

The physical equation is expressed as follows:

$$\begin{cases} \varepsilon_r = \dfrac{1-\mu^2}{E}\left(\sigma_r - \dfrac{\mu}{1-\mu}\sigma_\theta\right) \\ \varepsilon_\theta = \dfrac{1-\mu^2}{E}\left(\sigma_\theta - \dfrac{\mu}{1-\mu}\sigma_r\right) \end{cases}, \tag{10}$$

where μ is Poisson's ratio.

Under the plain strain condition, the intermediate principal stress influence coefficient b $(0 \le b \le 1)$ reflects the influence degree of the intermediate principal stress on the rock failure. When the material is under yield and failure state, b is approximate to 1, and generally, $b = 1$. In this study, $b = 1$ was taken, and the unified strength criterion under the plane strain condition can then be obtained as follows:

$$\sigma_1 - A_{i,\varphi}\sigma_3 - B_{i,\varphi} = 0, \tag{11}$$

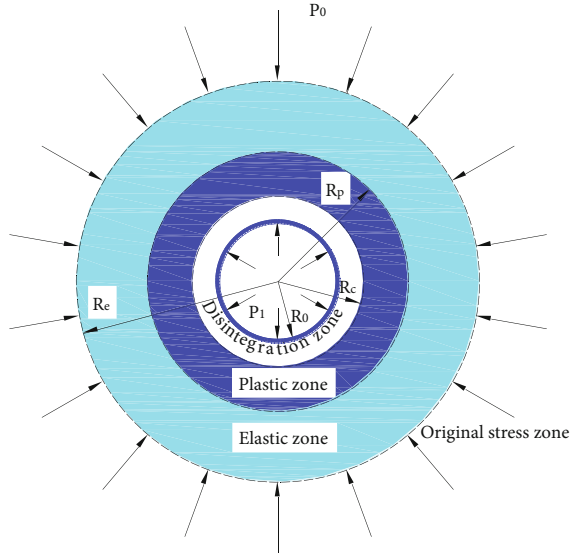

Figure 2: Mechanical model of circular roadway.

where $A_{i,\phi} = 2 + 2b - \alpha_i{}_{\phi} b/\alpha_i{}_{\phi}(2 + b)$, σ_c is the compressive strength of rock, and $\alpha_{i,\varphi}$ is the compressive strength ratio of the rock.

Under the nonassociated flow rule, the stress boundary conditions and contact conditions are as follows:

$$\begin{cases} r \longrightarrow \infty \quad \sigma_r^e = p_0 \quad u_e = 0 \\ r = R_p \quad \sigma_r^e = \sigma_r^p \quad u_e = u_p \\ r = R_c \quad \sigma_r^p = \sigma_r^c \quad u_p = u_c \\ r = R_0 \quad \sigma_r^c = p_1 \end{cases}. \tag{12}$$

Furthermore, through simultaneous Equations (8)–(10) and the different boundary conditions in Equation (12), the stress and deformation in the elastic, plastic, and disintegration zones, as well as the scopes of plastic and disintegration zones, can be solved by reference to literature [21].

3. Mechanical Response of Pressure Relief in Deep Roadway

3.1. Roadway Pressure Relief-Disturbed Zone Analysis of Surrounding Rock. Generally, the zone with a stress change of smaller than 5% is not affected by the excavation, and it is referred to as the stress zone of primary rock. The zone with the stress change of greater than 5%, which is affected by the excavation, is called the disturbed zone (the radius of the disturbed zone is r'), as shown in Figure 4.

r' is within the elastic zone, and the stress and radius of the disturbed zone are solved as follows:

$$\begin{aligned} \sigma_r^e &= p_0 - \left(p_0 - \sigma_R^p\right)\left(\frac{R_p}{r'}\right)^2 = 0.95p_0, \\ \mathrm{r}' &= 2\sqrt{5}R_p\sqrt{1 - \frac{\sigma_R^p}{p_0}}, \end{aligned} \tag{13}$$

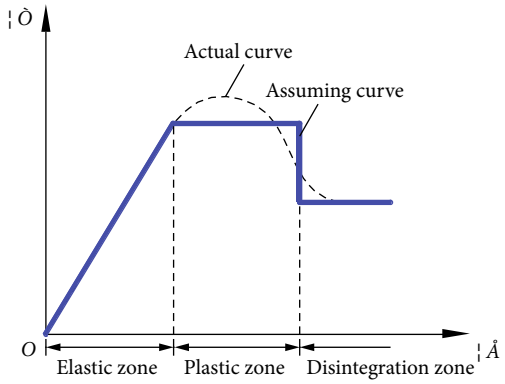

Figure 3: Stress–strain curves of rock deformation failure and zoning plan.

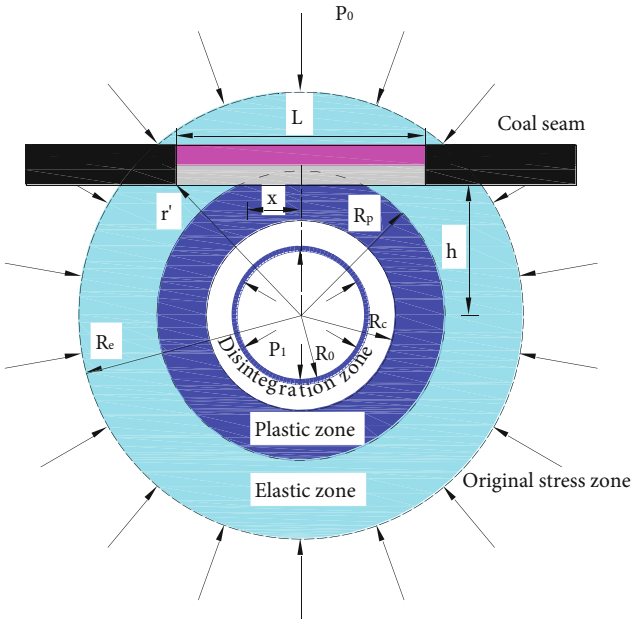

Figure 4: Pressure relief zoning model of floor roadway.

where $\sigma^p{}_R$ is the contact stress at the elastic–plastic interface, and it is calculated according to literature [21].

For the floor roadway in the outburst coal seam, its spacing with the overlying coal seam is generally greater than 7 m, that is, the coal seam is usually located within the elastic–plastic zone of the surrounding rock in the floor roadway. When $R_p < h < r^{'}$, the coal seam is located at the elastic zone and influenced by the roadway excavation; the horizontal stress change is as follows:

$$\begin{cases} \sigma_r^e = p_0 - \dfrac{(p_0 - \sigma_R^p)R_p{}^2}{h^2 + x^2} \\ \sigma_\theta^e = p_0 + \dfrac{(p_0 - \sigma_R^p)R_p{}^2}{h^2 + x^2} \end{cases}. \tag{14}$$

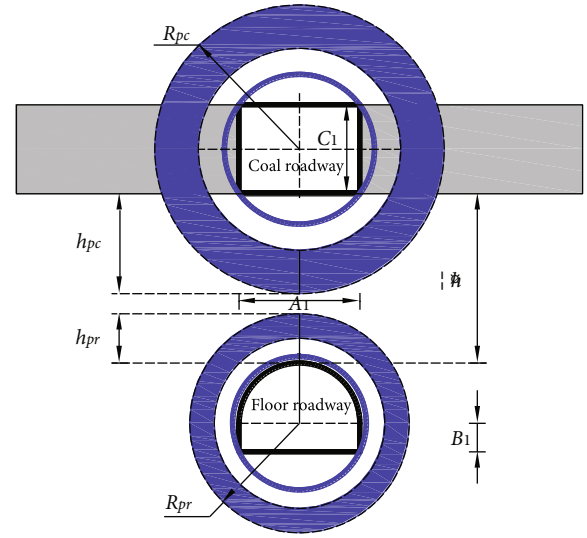

Figure 5: Schematic of surrounding rock deformation in double-roadway excavation.

When $R_c < h < R_p$, the coal seam is seated in the plastic and elastic zones. Under the influence of roadway excavation, the stress change in the horizontal direction is

$$\begin{cases} \sigma_r^p = (\sigma_R^p + D_p)\left(\dfrac{h^2 + x^2}{R_p{}^2}\right)^{\frac{A_p{}_{\phi}-1}{2}} - D_p \quad \left(0 \le x \le \sqrt{R_p{}^2 - h^2}\right) \\ \sigma_\theta^p = A_p(\sigma_R^p + D_p)\left(\dfrac{h^2 + x^2}{R_p{}^2}\right)^{\frac{A_p\&\phi-1}{2}} - D_p \quad \left(0 \le x \le \sqrt{R_p{}^2 - h^2}\right) \\ \sigma_r^e = p_0 - (p_0 - \sigma_R^p)\left(\dfrac{R_p{}^2}{h^2 + x^2}\right) \quad \left(\sqrt{R_p{}^2 - h^2} \le x \le \sqrt{r'^2 - h^2}\right) \\ \sigma_\theta^e = p_0 + (p_0 - \sigma_R^p)\left(\dfrac{R_p{}^2}{h^2 + x^2}\right) \quad \left(\sqrt{R_p{}^2 - h^2} \le x \le \sqrt{r'^2 - h^2}\right) \end{cases}, \tag{15}$$

where $D_p = B_p{}_{\phi}/A_p{}_{\phi} - 1$, and $A_{p,\psi} = 2 + 2b - \alpha_p{}_{\psi}b/\alpha_p{}_{\psi}(2 + b)$, which can be calculated according to literature [21].

When the coal seam is in the elastic and elastic–plastic zones, the minimum bottom stress is $\sigma 0_0{}_R^p R_p/h^2{}_{rmin}$ and $\sigma_{R_p}^p h/R_p{}^{A_{p,\psi}-1}{}_{p_{rmin}}$, respectively, and the horizontal disturbed area of the coal seam is $L = 2l = 2\sqrt{r'^2 - h^2}$.

3.2. Pressure Relief Mechanism of Short-Distance Floor Roadway for Coal Seam. The formulas for the vertical stress and displacement changes of the coal seam in the disturbed zone can be obtained through the coordinate transformation of elastic mechanics. For the axisymmetric problem, the coordinate transformation formula can be

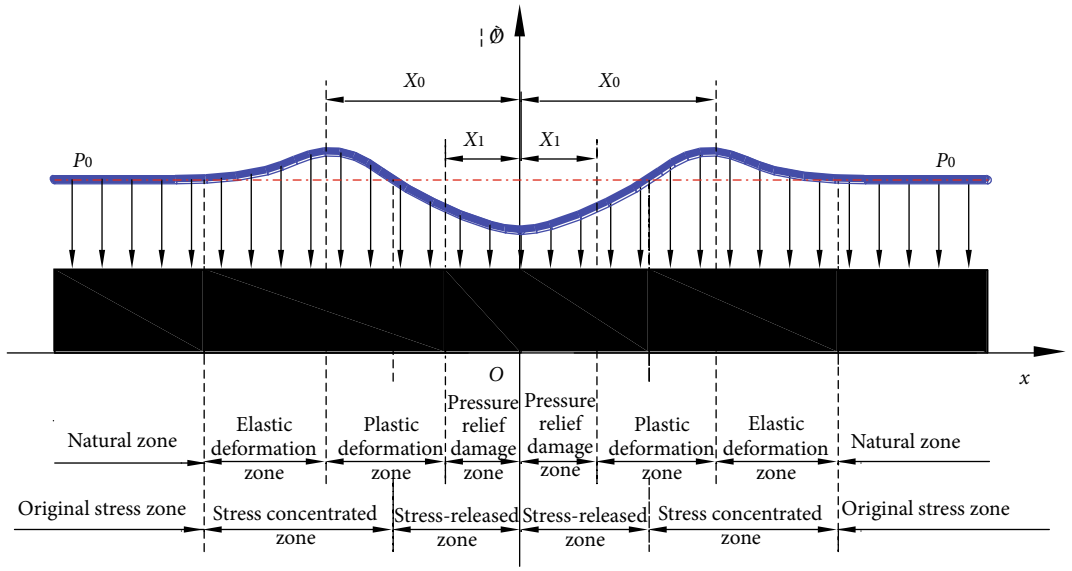

Figure 6: Mechanical model of pressure relief and permeability enhancement zones at coal seam.

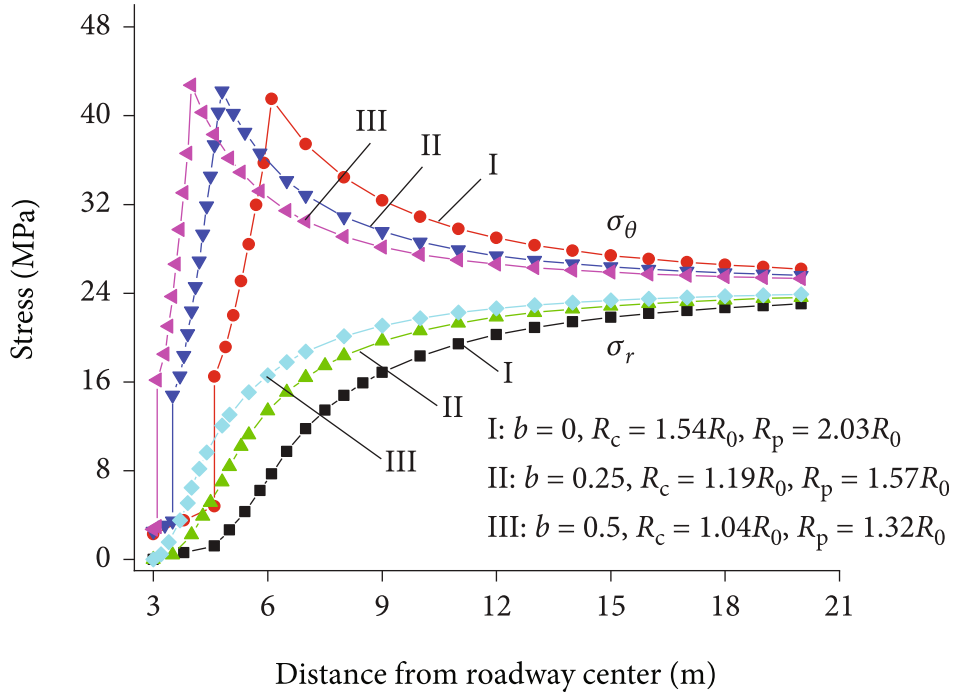

Figure 7: Stress distribution curve of surrounding rock in roadway.

simplified into the following form:

$$\begin{cases} \sigma_x = \sigma_r \sin^2\varphi + \sigma_\theta \cos^2\varphi \\ \sigma_y = \sigma_r \cos^2\varphi + \sigma_\theta \sin^2\varphi \\ u_x = u_r \sin\varphi \\ u_y = u_r \cos\varphi \end{cases}, \tag{16}$$

where φ is the included angle between the radius r and the vertical direction.

When the coal seam is in the elastic zone, Equation (14) is substituted into the above equation to solve the stress and displacement of the coal seam in the short-distance disturbed zone as follows:

$$\begin{cases} \sigma_x = p_0 + \dfrac{(p_0 - \sigma_R^p)R_p^2}{(h^2 + x^2)^2}(h^2 - x^2) \\ \sigma_y = p_0 - \dfrac{(p_0 - \sigma_R^p)R_p^2}{(h^2 + x^2)^2}(h^2 - x^2) \\ u_x = \dfrac{(p_0 - \sigma_R^p)R_p^2 x}{2G(h^2 + x^2)} \\ u_y = \dfrac{(p_0 - \sigma_R^p)R_p^2 h}{2G(h^2 + x^2)} \end{cases}. \tag{17}$$

3.3. Reasonable Position Criterion for Short-Distance Floor Roadway to Be Depressurized. After the overlying coal roadway of the floor roadway is excavated, the surrounding rock will experience secondary pressure relief. To prevent the outburst and guarantee the stability of surrounding rock, no through cracks should be formed at the rock pillar on the roadway roof, and the reasonable position model is shown in Figure 5.

As shown in Figure 5, the judgment criteria for the failure depths h_{pr} and h_{pc} of floor roadway and its overlying coal roadway for the rock mass, as well as the reasonable distance between the right-angular semicircular floor roadway and the coal seam, can be obtained as follows:

$$\begin{cases} h_{Pr} = \delta \cdot R_{Pr} - (C_1 - B_1) \\ h_{Pc} = \delta \cdot R_{Pc} - \dfrac{C_1}{2} \end{cases}, \tag{18}$$

$$\Delta h \geq \delta \cdot (R_{pr} + R_{pc}) - \left(\frac{3}{2}C_1 - B_1\right), \tag{19}$$

where δ is the superposition coefficient of the secondary pressure relief effect, which can be statistically analyzed through the field monitoring or calculated through the simulation.

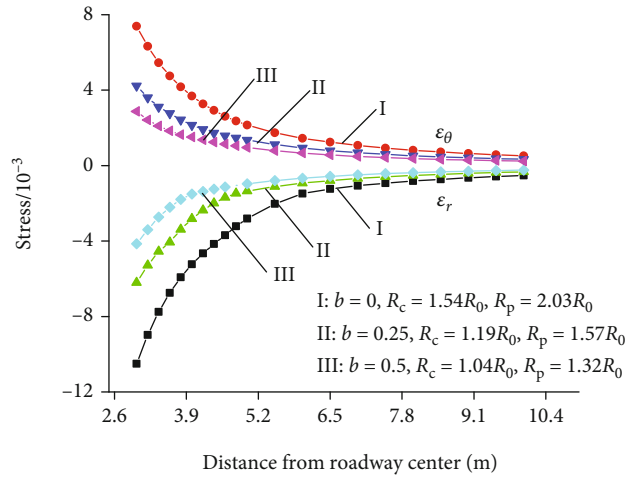

Figure 8: Strain distribution curve of surrounding rock in roadway.

4. Pressure Relief and Permeability Enhancement Mechanism of Floor Roadway at Deep Coal Roadway Strips

4.1. Pressure Relief and Zonal Disintegration Analysis of Floor Roadway at Coal Roadway Strips. After the short-distance floor roadway is excavated, the vertical stress at the coal seam rightly above the roadway is released. The original three-directional stress equilibrium of the coal mass is destructed, and the ultimate strength of the coal mass can be easily reached in the deep roadway, thereby leading to yield failure. Subsequently, the concentrated stress is transferred to the two sides to form a zoning model, as shown in Figure 6.

The vertical stress in the pressure relief damaged zone is obviously reduced. In this zone, the cracks are significantly developed in the coal mass, and it is called effective pressure relief zone, extending at the two sides X_1 of the center line in the roadway. The coal mass in the plastic deformation zone will experience minor deformation and cracking. Thus, the gas permeability coefficient is obviously enhanced, and it is called effective permeability enhancement zone, extending at the two sides X_0 of the center line in the roadway.

When the horizontal distance satisfies $x \leq h$, the first, second, and third principal stresses are σ_x, σ_z, and σ_y, respectively. Then,

$$\frac{\alpha_c}{1+b}(\sigma_x + b\sigma_z) - \sigma_y = \alpha\sigma_c. \tag{20}$$

After the floor roadway is excavated, the original adsorbed gas in the upper coal seam is transformed into free gas, the gas stress in the coal seam will be increased, whereas the uniaxial compressive strength will be reduced, which conforms to the following relation [4]:

$$\sigma_c = A_2 + B_2 \cdot p, \tag{21}$$

where A_2 and B_2 are the parameters related to the coal mass.

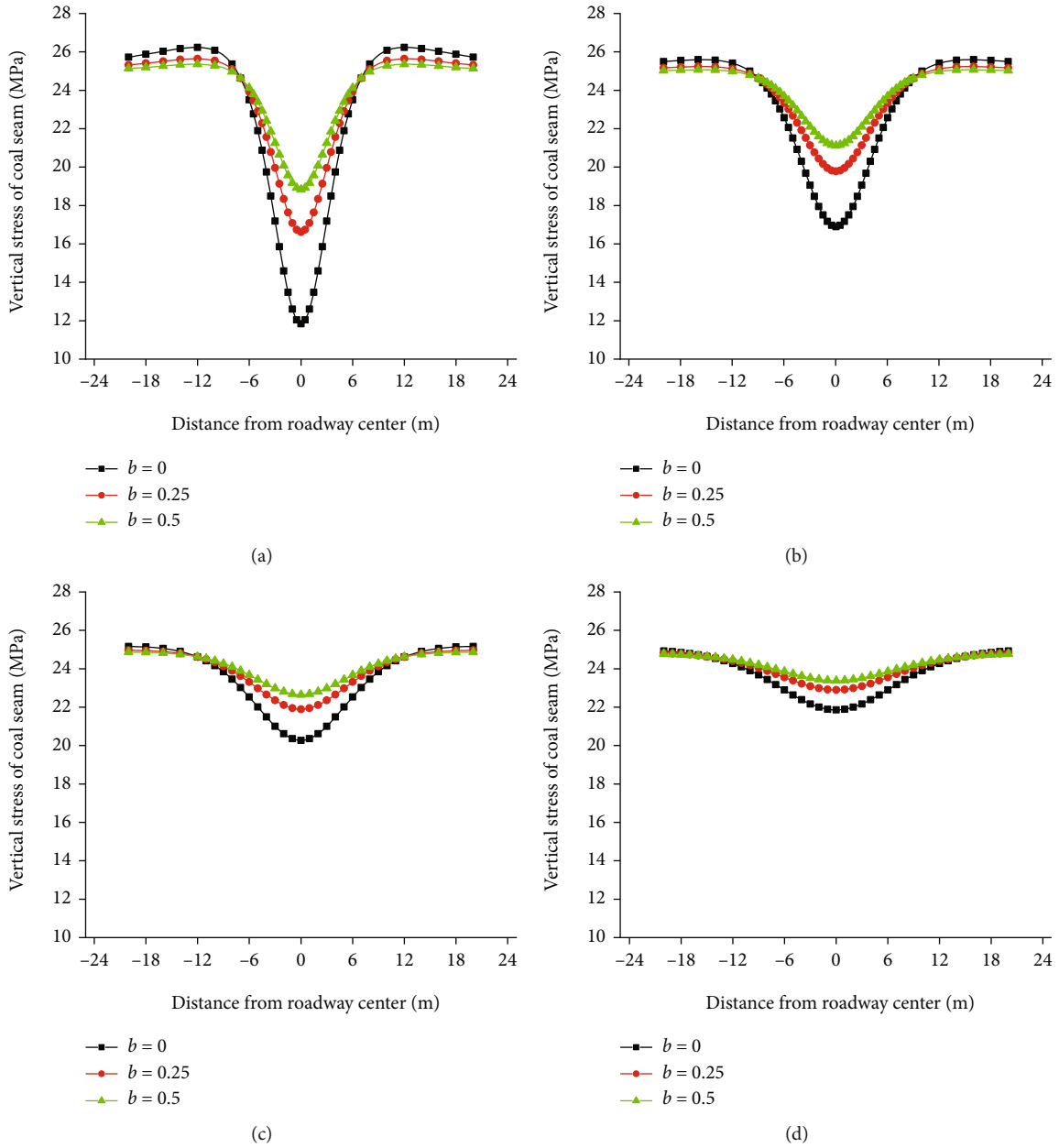

Figure 9: Continued.

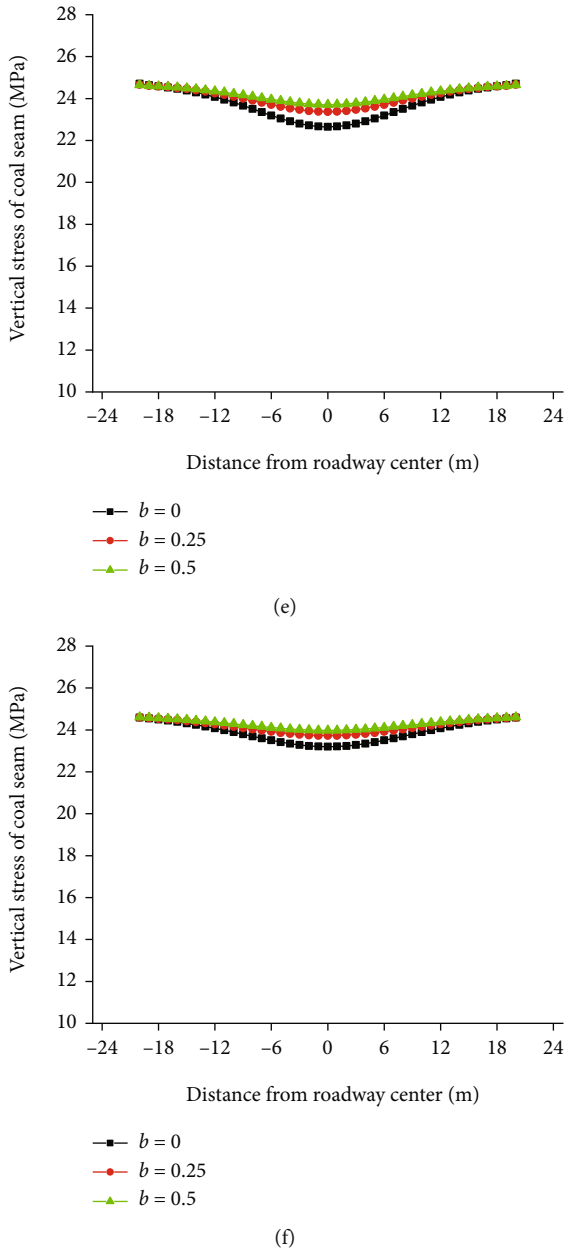

Figure 9: Vertical stress of coal seam during the excavation of floor roadways under different spacings.

Table 1: Pressure relief coefficients (%) at the center line of the roadway and coal seams at two sides.

b	Vertical distance h/m					
	7	9	12	15	18	21
0	52.0–4.6	31.4–5.0	17.7–4.7	11.3–4.9	7.8-2.7	5.8–2.3
0.25	32.6–2.9	19.7–3.2	11.1–2.7	7.1–3.1	4.9-2.2	3.6–2.0
0.5	23.6–2.1	14.3–2.2	8.0–2.2	5.1–2.2	3.6-2.0	2.6–1.9
Two sides	6 m	7 m	8 m	8 m	5 m	5 m

Table 2: Radius of plastic zone in the roadway under different principal stress coefficients.

Roadway name	Roadway shape	Equivalent radius R_0/m	Radius of plastic zone R_p/m		
			$b = 0$	$b = 0.25$	$b = 0.5$
Floor roadway	Right-angular semicircular arch	2.24	4.55	3.52	2.96
Overlying coal roadway	Rectangular	2.47	5.01	3.88	3.26

Table 3: Pressure relief effect of the overlying coal seam in the floor roadway at different positions.

h /m	Effective pressure relief zone $X1$/m	Effective permeability enhancement zone $X0$/m	Permeability enhancement ratio	Gas permeability enhancement ratio	Pressure relief effect
7	4.3	12.1	0.28–6.06	11.1–239.3	
9	3.5	15.4	0.17–2.26	6.7–89.2	Obvious
12	1.2	20.5	0.09–0.94	3.6–37.1	
15	0.3	20.7	0.06–0.23	2.4–9.1	
18	0	20.5	0.03–0.14	1.2–5.5	Unobvious
21	0	20.4	0.02–0.04	0.8–1.6	

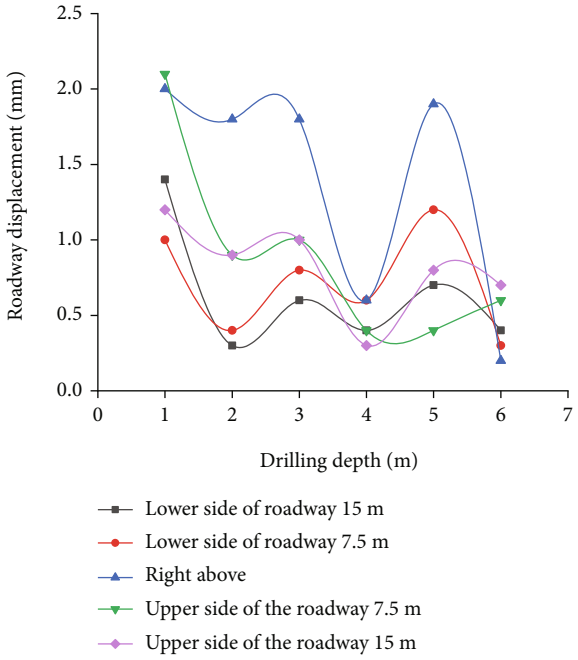

Figure 10: Displacement of surrounding rock in 213 floor roadway.

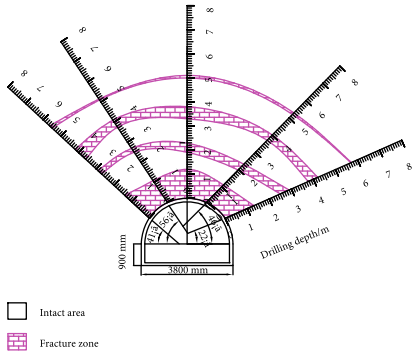

Figure 11: Failure of surrounding rock in 213 floor roadway.

Substituting Equation (17) and (21) into Equation (20) yields the following:

$$\frac{1-\sin\varphi}{(1+b)(1+\sin\varphi)}\left[P_0+\frac{(P_0-\sigma_R^p){R_p}^2}{\left(h^2+{X_1}^2\right)^2}\left(h^2-{X_1}^2\right)+b\sigma_z\right]-P_0+\frac{(P_0-\sigma_R^p){R_p}^2}{\left(h^2+{X_1}^2\right)^2}\left(h^2-{X_1}^2\right)=\frac{1-\sin\varphi}{1+\sin\varphi}(A_2+B_2\cdot p). \tag{22}$$

According to the change laws of the uniaxial compressive strength of gassy coal seam, the width X_1 of the pressure relief damaged zone of short-distance floor for the overlying coal seam can be solved by combining the layout conditions of the floor roadway, the coal mass-related parameters at the overlying coal seam, and Equation (22).

The horizontal distance X_0 of the effective pressure zone is the horizontal distance when the vertical stress σ_y reaches the maximum value. As the analytical expression of σ_y in Equation (17) is complicated, the maximum value of σ_y and horizontal distance X_0 of effective pressure relief zone can be calculated via MATLAB.

4.2. Pressure Relief and Permeability Enhancement Mechanism of Floor Roadway at Coal Roadway Strips. According to the stress unloading experiment of gassy coal samples under constant confining pressure and atmospheric pressure, the fitting relation between permeability K and $\sigma_1 - \sigma_3$ is as follows [4]:

$$K = A_3 \cdot e^{B_3\cdot(\sigma_1-\sigma_3)}, \tag{23}$$

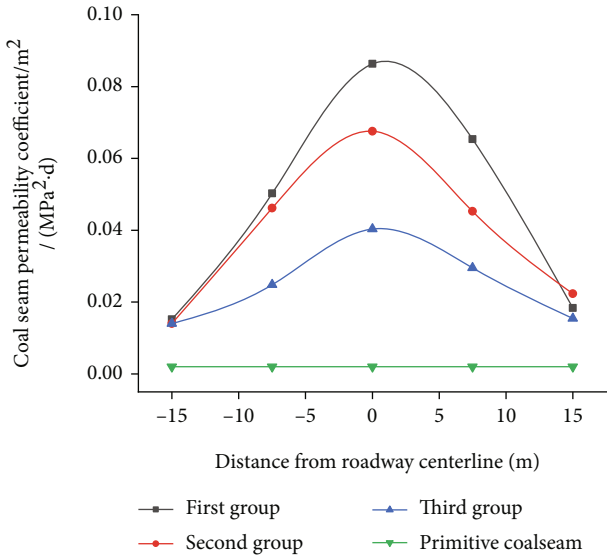

Figure 12: Gas permeability coefficient of overlying coal seam in 213 floor roadway.

where A_3 and B_3 are the parameters related to coal mass, stress, and gas.

As indicated by Equation (17) and the stress analysis of the surrounding rock, when $x < h$, the first and third principal stresses are σ_x and σ_y, respectively; when $x > h$, the first and third principal stresses are σ_y and σ_x, respectively. Therefore, the formulas of permeability K and $\sigma_1-\sigma_3$ can be organized as follows:

$$\begin{cases} K = A_3 \cdot e^{2B_3 \cdot \left(p_0 - \sigma_R^p\right)\left(h^2 - x^2\right)R_p^2/\left(h^2+x^2\right)^2} & x < h \\ K = A_3 \cdot e^{-2B_3 \cdot \left(p_0 - \sigma_R^p\right)\left(h^2 - x^2\right)R_p^2/\left(h^2+x^2\right)^2} & x > h \end{cases}. \quad (24)$$

The difficulty of coal seam gas extraction is generally expressed by the gas permeability coefficient, which also characterizes the resistance formed by the coal seam to the gas flow. According to the relationship between the gas permeability coefficient of the coal seam and the permeability of the pressure-bearing coal sample [27], the relationship between the gas permeability coefficient of the coal seam and the stress change can be further acquired, as shown as follows:

$$\begin{cases} \lambda = \dfrac{A_3}{2\rho p_n} \cdot e^{2B_3 \cdot \left(p_0 - \sigma_R^p\right)\left(h^2 - x^2\right).R_p^2/\left(h^2+x^2\right)^2} & x < h \\ \lambda = \dfrac{A_3}{2\rho p_n} \cdot e^{-2B_3 \cdot \left(p_0 - \sigma_R^p\right)\left(h^2 - x^2\right).R_p^2/\left(h^2+x^2\right)^2} & x > h \end{cases}, \quad (25)$$

where ρ represents the absolute viscosity of gas, 1.08×10^{-8} N·s/cm^2; and P_n denotes a standard atmospheric pressure, 0.1013 MPa.

5. Pressure Relief and Permeability Enhancement Practice of Floor Roadway at Deep Coal Roadway Strips

5.1. Engineering Trial Calculation. The parameters used in the calculated example were the measured parameters of 213 floor coal rock stratum in Qujiang Coal Mine. The burial depth of 213 floor roadway was about 980 m, the roadway size was 4.0 m × 3.0 m, the wall height was 1.0 m, and the thickness of overlying B_4 coal seam was 3 m. According to the stress of the primary rock and the experiment, the vertical and horizontal stress components were 24.92 MPa and 24.35 MPa, respectively, and $P_0 = 24.6$ MPa; the Poisson's ratio, initial friction angle, initial cohesion, residual internal friction angle, and residual cohesion of rock were $\mu = 0.25$, $\varphi_p = 35°$, $c_p = 3$ MPa, $\varphi_c = 20°$, and $c_p = 0.8$ MPa, respectively, $\sigma_c = -1.576p + 24.77$ and $K_0 = 2.7191 \cdot e^{-0.09\cdot(\sigma_1-\sigma_3)}$.

The equivalent elasticity modulus of the rock and the equivalent excavation radius of the floor roadway were calculated as $E = 15.0$ GPa and $R_0 = 2.24$ m, respectively. When the intermediate principal stress coefficient b was taken as 0.75 and 1, the calculation results showed that no disintegration zone appeared in the roadway, which did not conform to the engineering practice. By combining literature [22], the stress, deformation, plastic zone, and permeability (Figures 7–9, Tables 1–3) were analyzed under $b = 0$, 0.25, and 0.5, respectively.

As shown in Figures 7–9, the circumferential stress of the surrounding rock in the roadway under different values of b was initially increased and then reduced, reaching the maximum value at the elastic–plastic interface. With the increase in the coefficient b, the circumferential stress reached the peak value at a closer distance from the roadway surface. Under different values of b, the radial stress presented a monotonic increasing trend and reached the stress of the primary rock at an infinite distance. At the same vertical distance in the elastic zone, the radial stress of the rock increased with coefficient b, whereas the circumferential stress showed an opposite trend. The absolute value of stain was gradually reduced with the distance; thus, the strain was obviously affected by coefficient b.

As shown in Figure 9 and Table 1, the pressure relief coefficient had the same change law as the vertical stress. The vertical stress of the coal seam was gradually reduced from the center line of the roadway toward the two sides, and it was also gradually reduced with the increase in the intermediate principal stress coefficient b and vertical distance h.

As shown in Table 2, the radius of the plastic zone in the roadway was gradually reduced with the increase in the intermediate principal stress coefficient b. $b = 0$ was taken to ensure the safety of distance arrangement. When $\delta = 1$, the minimum reasonable distance arranged in the floor roadway could be obtained as $\Delta h = 6.21$ m.

As shown in Table 3, with the increase in the distance from the floor roadway to the coal seam, the pressure relief effect was gradually weakened. When the distance reached

12 m, the pressure relief effect was not evident. By combining Equation (19), the pressure relief and permeability enhancement effect was significant when the roadway was arranged within 10.6 m from the coal seam.

5.2. Engineering Practice. Similarly, an engineering practice was performed in the 213 coal roadway of Qujiang Coal Mine. This floor roadway was arranged at 9.0 m away from the coal seam. The displacement of surrounding rock was measured using a DW-6 multipoint displacement meter. The failure status of surrounding rock was detected via YTJ20 rock strata detection recorder. The gas permeability coefficient of the coal seam was measured using a test drill hole, and the test results are displayed in Figures 10–12.

The field measurement showed that the "wave crest" and "trough" of the surrounding rock displacement in the roadway alternately appeared. An obvious pressure relief effect was achieved when the surrounding rock displacement was 1.2–2.1 cm and the expansion rate was 1.3‰–2.3‰. The zonal disintegration phenomenon occurred to the surrounding rock in the roadway. Four disintegration zones appeared inside the roadway from the wall, their maximum scope of influence was 5.7 m, and the investigation result was basically consistent with the theoretical analysis. The gas permeability coefficient in the coal seam under pressure relief was obviously enlarged in comparison to the original coal seam, being increased by 8.1–54.7 times in different zones. The permeability enhancement effect of short-distance floor roadway on the overlying coal roadway strip was significant, which highly coincided with the theoretical analysis.

6. Conclusion

(1) An equivalent mechanical model of the surrounding rock in deep roadway was established. The analytical solutions of deep roadway excavation to the pressure relief-induced stress and deformation at overlying short-distance coal roadway strips were obtained through the unified strength criterion and nonassociated flow rule. Next, the criterion for determining the reasonable position of floor roadway was constructed

(2) A mechanical model of short-distance floor roadway for the zonal pressure relief and permeability enhancement in the overlying coal seam was established. The expressions of stress and permeability changes at the coal roadway strips in the elastic and elastic–plastic zones of the surrounding rock in the roadway were given

(3) The engineering calculation example indicated that the intermediate principal stress coefficient exerted obvious effects on the stress and strain of the surrounding rock in the roadway. The vertical stress and vertical displacement of the overlying coal seam were gradually reduced with the increase in the intermediate principal stress coefficient and vertical distance of the floor roadway. The minimum reasonable distance arranged for the 213 floor roadway in Qujiang Coal Mine was 6.21 m, and the position of effective pressure relief should be located within 10.6 m from the coal seam floor

(4) The field practice manifested that the deep floor roadway exerted obvious pressure relief and permeability enhance effect on the overlying short-distance coal roadway strips. The investigation results were basically identical with the theoretical analysis results. Thus, the pressure relief and permeability enhancement method of short-distance floor roadway at deep coal roadway strips was feasible

Data Availability

The known data in this paper come from practical engineering case data, which are reliable and available.

Conflicts of Interest

The authors declare that they have no conflicts of interest.

Acknowledgments

This work is financially supported by the National Natural Science Foundation of China (Nos. 52074008, 52074007, and 52004005), the Anhui Provincial Natural Science Foundation (Nos. 2008085ME142 and 2008085QE222), the Anhui Collaborative University Innovation Project (GXXT-2020-056), the China Postdoctoral Science Foundation (2021 M691185), Open Research Fund Project of Key Laboratory of Safety and High-Efficiency Coal Mining of Ministry of Education (JYBSYS2019208), and the Independent Research Fund of The State Key Laboratory of Mining Response and Disaster Prevention and Control in Deep Coal Mines (Anhui University of Science and Technology, No. SKLMRDPC19ZZ012).

References

[1] L. Yuan, "Strategic thinking of simultaneous exploitation of coal and gas in deep mine," *Journal of China Coal Society*, vol. 41, no. 1, pp. 1–6, 2016.

[2] H. P. Xie, M. G. Qian, S. P. Peng, S. S. Hu, Y. Q. Cheng, and H. W. Zhou, "Sustainable capacity of coal mining and its strategic plan," *Engineering Science*, vol. 13, no. 6, pp. 44–50, 2011.

[3] C. J. Lian, C. M. Guo, Z. Y. Deng, and H. Y. Ma, "Spatial gas control technology and application of first mining protective layer of coal seam group with high gas outburst," *Coal Mining*, vol. 24, no. 1, pp. 124–127, 2019.

[4] X. Cheng, G. M. Zhao, Y. M. Li, X. R. Meng, C. L. Dong, and W. S. Xu, "Study on relief-pressure antireflective effect and gas extraction technology for mining soft rock protective seam," *Journal of Mining & Safety Engineering*, vol. 35, no. 5, pp. 1045–1053, 2018.

[5] M. J. Zhang, J. J. Hua, and J. T. Hua, "Anti-burst technology of gas strip in pre-extracted coal roadway with single coal seam floorway," *Coal Mine Safety*, vol. 42, no. 6, pp. 30–32, 2011.

[6] L. Yuan, "Control of coal and gas outbursts in Huainan mines in china: a review," *Journal of Rock Mechanics and Geotechnical Engineering*, vol. 8, no. 4, pp. 559–567, 2016.

[7] D. J. Lei, C. W. Li, Z. M. Zhang, and Y. G. Zhang, "Coal and gas outburst mechanism of the "Three Soft" coal seam in Western Henan," *Mining Science and Technology*, vol. 20, no. 5, pp. 712–717, 2010.

[8] C. H. Du and R. J. Feng, "Study on hydraulic creaming technology in low permeability and soft friable thick coal seam," *Coal Science and Technology*, vol. 47, no. 4, pp. 152–156, 2019.

[9] F. Cai and Z. G. Liu, "Simulation and experimental research on upward cross-seams hydraulic fracturing in deep and low-permeability coal seam," *Journal of China Coal Society*, vol. 41, no. 1, pp. 113–119, 2016.

[10] P. Li, K. Wang, Y. F. Jiang, and J. Q. Gou, "Applied study on hydraulic reaming technology of mining seam in Hongling Mine," *Coal Science and Technology*, vol. 43, no. 7, pp. 69–73, 2015.

[11] X. J. Jian and F. Cai, "Study on the technology of hydraulic fracturing strengthening and deepening in deep low permeability coal seam," *Safety in Coal Mines*, vol. 48, no. 10, pp. 76–79, 2017.

[12] J. F. Zhao, "Study on the technology of hydraulic punching strengthening and deepening in deep low permeability coal seam," *Coal Technology*, vol. 34, no. 1, pp. 179–181, 2015.

[13] Y. H. Zhou, X. R. Luo, L. L. Wu, and J. N. Xie, "Research status and new technology of anti-pressure and pressure relief of low permeability coal seam," *Mining Research and Development*, vol. 32, no. 1, pp. 23–25, 2012.

[14] F. Cai, Z. G. Liu, C. J. Zhang, and B. Q. Lin, "Numerical simulation of deep hole pre-splitting blasting in high gas permeability coal seam," *Journal of China Coal Society*, vol. 5, pp. 499–503, 2007.

[15] H. P. Xie, F. Gao, and Y. Ju, "Research and development of rock mechanics in deep ground engineering," *Chinese Journal of Rock Mechanics and Engineering*, vol. 34, no. 11, pp. 2161–2178, 2015.

[16] H. P. Xie, "Research review of the state key research development program of China: deep rock mechanics and mining theory," *Journal of China Coal Society*, vol. 44, no. 5, pp. 1283–1305, 2019.

[17] Q. Zhang, S. L. Wang, and X. R. GE, "Elastoplastic analysis of strain softening of surrounding rock of circular roadway," *Journal of Rock Mechanics and Engineering*, vol. 29, no. 5, p. 1035, 2010.

[18] B. S. Jiang, L. Yang, and L. P. Lin, "Stress analysis of fractured surrounding rock based on Hoek-Brown criterion," *Journal of Solid Mechanics*, vol. 32, no. S1, pp. 300–305, 2011.

[19] X. B. Zhang, G. M. Zhao, and X. R. Meng, "Plastic zone analysis of surrounding rock of circular roadway in non-uniform stress field based on the unified strength criterion of rock nonlinearity," *Journal of Safety and Environment*, vol. 13, no. 3, pp. 202–206, 2013.

[20] B. S. Jiang, Q. Zhang, Y. N. He, and L. J. Han, "Elastoplastic analysis of surrounding rock of deep circular roadway fracture," *Journal of Rock Mechanics and Engineering*, vol. 5, pp. 982–986, 2007.

[21] L. Chen, X. B. Mao, M. Li, and Y. L. Chen, "Elastoplastic analysis of cracked surrounding rock in deep roadway based on Drucker-Prager criterion," *Journal of China Coal Society*, vol. 42, no. 2, pp. 484–491, 2017.

[22] C. G. Zhang, C. L. Zhang, F. Zhou, and Q. Yan, "Study on the strength theory effect of elastoplastic analysis of circular tunnels," *Chinese Journal of Geotechnical Engineering*, vol. 40, no. 8, pp. 1449–1456, 2018.